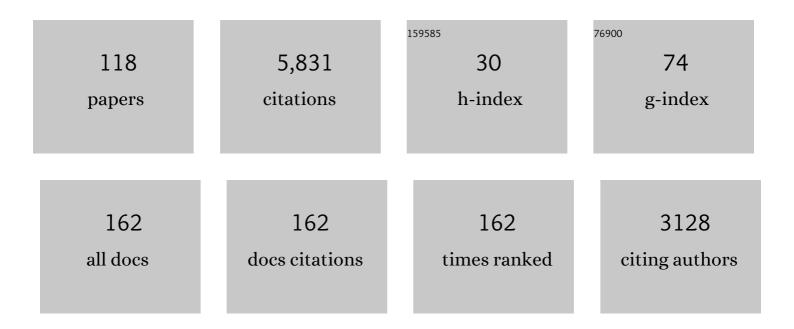
Harald Schuh

List of Publications by Year in descending order

Source: https://exaly.com/author-pdf/211787/publications.pdf Version: 2024-02-01



#	Article	IF	CITATIONS
1	Global Mapping Function (CMF): A new empirical mapping function based on numerical weather model data. Geophysical Research Letters, 2006, 33, .	4.0	1,010
2	Troposphere mapping functions for GPS and very long baseline interferometry from European Centre for Mediumâ€Range Weather Forecasts operational analysis data. Journal of Geophysical Research, 2006, 111, .	3.3	794
3	Short Note: A global model of pressure and temperature for geodetic applications. Journal of Geodesy, 2007, 81, 679-683.	3.6	530
4	Accuracy and reliability of multi-GNSS real-time precise positioning: GPS, GLONASS, BeiDou, and Galileo. Journal of Geodesy, 2015, 89, 607-635.	3.6	521
5	Precise positioning with current multi-constellation Global Navigation Satellite Systems: GPS, GLONASS, Galileo and BeiDou. Scientific Reports, 2015, 5, 8328.	3.3	264
6	VLBI: A fascinating technique for geodesy and astrometry. Journal of Geodynamics, 2012, 61, 68-80.	1.6	228
7	ICGEM – 15 years of successful collection and distribution of global gravitational models, associated services, and future plans. Earth System Science Data, 2019, 11, 647-674.	9.9	172
8	Achievements of the Earth orientation parameters prediction comparison campaign. Journal of Geodesy, 2010, 84, 587-596.	3.6	106
9	Retrieving of atmospheric parameters from multiâ€GNSS in real time: Validation with water vapor radiometer and numerical weather model. Journal of Geophysical Research D: Atmospheres, 2015, 120, 7189-7204.	3.3	85
10	Three-frequency BDS precise point positioning ambiguity resolution based on raw observables. Journal of Geodesy, 2018, 92, 1357-1369.	3.6	81
11	Global Ionosphere Maps of VTEC from GNSS, satellite altimetry, and formosat-3/COSMIC data. Journal of Geodesy, 2011, 85, 975-987.	3.6	75
12	Multi-technique comparison of troposphere zenith delays and gradients during CONT08. Journal of Geodesy, 2011, 85, 395-413.	3.6	74
13	Real-time retrieval of precipitable water vapor from GPS and BeiDou observations. Journal of Geodesy, 2015, 89, 843-856.	3.6	73
14	Multi-technique comparison of tropospheric zenith delays derived during the CONT02 campaign. Journal of Geodesy, 2006, 79, 613-623.	3.6	67
15	Initial Assessment of Precise Point Positioning with LEO Enhanced Global Navigation Satellite Systems (LeGNSS). Remote Sensing, 2018, 10, 984.	4.0	66
16	LEO enhanced Global Navigation Satellite System (LeGNSS) for real-time precise positioning services. Advances in Space Research, 2019, 63, 73-93.	2.6	65
17	The New Vienna VLBI Software VieVS. International Association of Geodesy Symposia, 2012, , 1007-1011.	0.4	58
18	Estimating the yaw-attitude of BDS IGSO and MEO satellites. Journal of Geodesy, 2015, 89, 1005-1018.	3.6	54

#	Article	IF	CITATIONS
19	Improving BeiDou real-time precise point positioning with numerical weather models. Journal of Geodesy, 2017, 91, 1019-1029.	3.6	53
20	Advanced technologies for satellite navigation and geodesy. Advances in Space Research, 2019, 64, 1256-1273.	2.6	52
21	Monte Carlo simulations of the impact of troposphere, clock and measurement errors on the repeatability of VLBI positions. Journal of Geodesy, 2011, 85, 39-50.	3.6	48
22	Retrieving Precipitable Water Vapor From Shipborne Multiâ€GNSS Observations. Geophysical Research Letters, 2019, 46, 5000-5008.	4.0	46
23	Application of Kalman filtering in VLBI data analysis. Earth, Planets and Space, 2015, 67, .	2.5	44
24	Tropospheric delay parameters from numerical weather models for multi-GNSS precise positioning. Atmospheric Measurement Techniques, 2016, 9, 5965-5973.	3.1	42
25	Effect of different tropospheric mapping functions on the TRF, CRF and position time-series estimated from VLBI. Journal of Geodesy, 2007, 81, 409-421.	3.6	40
26	Troposphere gradients from the ECMWF in VLBI analysis. Journal of Geodesy, 2007, 81, 403-408.	3.6	39
27	Using the Global Navigation Satellite System and satellite altimetry for combined Global Ionosphere Maps. Advances in Space Research, 2008, 42, 727-736.	2.6	38
28	Global morphology of ionospheric sporadic E layer from the FormoSat-3/COSMIC GPS radio occultation experiment. GPS Solutions, 2018, 22, 1.	4.3	38
29	New VLBI2010 scheduling strategies and implications on the terrestrial reference frames. Journal of Geodesy, 2014, 88, 449-461.	3.6	37
30	Estimating Integrated Water Vapor Trends From VLBI, GPS, and Numerical Weather Models: Sensitivity to Tropospheric Parameterization. Journal of Geophysical Research D: Atmospheres, 2018, 123, 6356-6372.	3.3	37
31	Effects of the 2nd order ionospheric terms on VLBI measurements. Geophysical Research Letters, 2005, 32, .	4.0	33
32	Rayâ€ŧraced tropospheric delays in VLBI analysis. Radio Science, 2012, 47, .	1.6	32
33	GNSS tropospheric gradients with high temporal resolution and their effect on precise positioning. Journal of Geophysical Research D: Atmospheres, 2016, 121, 912-930.	3.3	30
34	Free core nutation observed by VLBI. Astronomy and Astrophysics, 2013, 555, A29.	5.1	28
35	Combination of long time-series of troposphere zenith delays observed by VLBI. Journal of Geodesy, 2007, 81, 483-501.	3.6	26
36	Atmospheric Pressure Loading. Springer Atmospheric Sciences, 2013, , 137-157.	0.3	26

#	Article	IF	CITATIONS
37	Modeling thermal deformation of VLBI antennas with a new temperature model. Journal of Geodesy, 2007, 81, 423-431.	3.6	24
38	Earth Rotation Observed by Very Long Baseline Interferometry and Ring Laser. Pure and Applied Geophysics, 2009, 166, 1499-1517.	1.9	23
39	Tropospheric delay determination by Kalman filtering VLBI data. Earth, Planets and Space, 2015, 67, .	2.5	22
40	Improving integer ambiguity resolution for GLONASS precise orbit determination. Journal of Geodesy, 2016, 90, 715-726.	3.6	22
41	Very long baseline interferometry as a tool to probe the ionosphere. Radio Science, 2006, 41, n/a-n/a.	1.6	21
42	VLBI-derived troposphere parameters during CONT08. Journal of Geodesy, 2011, 85, 377-393.	3.6	21
43	Tidal Love and Shida numbers estimated by geodetic VLBI. Journal of Geodynamics, 2013, 70, 21-27.	1.6	21
44	Ray tracing technique for global 3-D modeling of ionospheric electron density using GNSS measurements. Radio Science, 2015, 50, 539-553.	1.6	20
45	Testing a new Free Core Nutation empirical model. Journal of Geodynamics, 2016, 94-95, 59-67.	1.6	20
46	Occurrence climatology of equatorial plasma bubbles derived using FormoSat-3 â^ COSMIC GPS radio occultation data. Annales Geophysicae, 2020, 38, 611-623.	1.6	20
47	GLONASS FDMA data for RTK positioning: a five-system analysis. GPS Solutions, 2021, 25, 1.	4.3	20
48	Correcting surface loading at the observation level: impact on global GNSS and VLBI station networks. Journal of Geodesy, 2019, 93, 2003-2017.	3.6	19
49	Structure Effects for 3417 Celestial Reference Frame Radio Sources. Astrophysical Journal, Supplement Series, 2019, 242, 5.	7.7	19
50	Sea-Ice Concentration Derived From GNSS Reflection Measurements in Fram Strait. IEEE Transactions on Geoscience and Remote Sensing, 2019, 57, 10350-10361.	6.3	18
51	High-resolution atmospheric angular momentum functions related to Earth rotation parameters during CONT08. Journal of Geodesy, 2011, 85, 425-433.	3.6	17
52	GPS derived Zenith Total Delay (ZTD) observed at tropical locations in South India during atmospheric storms and depressions. Journal of Atmospheric and Solar-Terrestrial Physics, 2015, 125-126, 1-7.	1.6	17
53	Asymmetric tropospheric delays from numerical weather models for UT1 determination from VLBI Intensive sessions on the baseline Wettzell–Tsukuba. Journal of Geodesy, 2010, 84, 319-325.	3.6	16
54	Universal time from VLBI single-baseline observations during CONT08. Journal of Geodesy, 2011, 85, 415-423.	3.6	16

#	Article	IF	CITATIONS
55	New approach for earthquake/tsunami monitoring using dense GPS networks. Scientific Reports, 2013, 3, 2682.	3.3	16
56	On the impact of local ties on the datum realization of global terrestrial reference frames. Journal of Geodesy, 2019, 93, 655-667.	3.6	16
57	Validating HY-2A CMR precipitable water vapor using ground-based and shipborne GNSS observations. Atmospheric Measurement Techniques, 2020, 13, 4963-4972.	3.1	16
58	THE SOURCE STRUCTURE OF 0642+449 DETECTED FROM THE CONT14 OBSERVATIONS. Astronomical Journal, 2016, 152, 151.	4.7	15
59	Realâ€Time Sensing of Precipitable Water Vapor From BeiDou Observations: Hong Kong and CMONOC Networks. Journal of Geophysical Research D: Atmospheres, 2018, 123, 7897-7909.	3.3	15
60	Short Period Variations In Earth Rotation As Seen By VLBI. Surveys in Geophysics, 2000, 21, 499-520.	4.6	14
61	Improving BeiDou precise orbit determination using observations of onboard MEO satellite receivers. Journal of Geodesy, 2017, 91, 1447-1460.	3.6	14
62	Multi-constellation GNSS orbit combination based on MGEX products. Advances in Geosciences, 0, 50, 57-64.	12.0	14
63	The Role of GNSS Vertical Velocities to Correct Estimates of Sea Level Rise from Tide Gauge Measurements in Greece. Marine Geodesy, 2017, 40, 297-314.	2.0	13
64	Characterization of GPS-TEC over African equatorial ionization anomaly (EIA) region during 2009–2016. Advances in Space Research, 2019, 63, 282-301.	2.6	13
65	VLBI2010: A Vision for Future Geodetic VLBI. , 2007, , 757-759.		13
66	An Improved Empirical Harmonic Model of the Celestial Intermediate Pole Offsets from a Global VLBI Solution. Astronomical Journal, 2017, 154, 166.	4.7	12
67	Improving Low Earth Orbit (LEO) Prediction with Accelerometer Data. Remote Sensing, 2020, 12, 1599.	4.0	12
68	On the consistency of the current conventional EOP series and the celestial and terrestrial reference frames. Journal of Geodesy, 2017, 91, 135-149.	3.6	11
69	Evidence of the <i>Gaia</i> –VLBI position differences being related to radio source structure. Astronomy and Astrophysics, 2021, 647, A189.	5.1	11
70	The effect of function-based and voxel-based tropospheric tomography techniques on the GNSS positioning accuracy. Journal of Geodesy, 2021, 95, 1.	3.6	11
71	A Global Terrestrial Reference Frame from simulated VLBI and SLR data in view of GGOS. Journal of Geodesy, 2017, 91, 723-733.	3.6	10
72	Performance Evaluation of VTEC GIMs for Regional Applications during Different Solar Activity Periods, Using RING TEC Values. Remote Sensing, 2021, 13, 1470.	4.0	10

#	Article	IF	CITATIONS
73	Observable quality assessment of broadband very long baseline interferometry system. Journal of Geodesy, 2021, 95, 1.	3.6	10
74	Improving VLBI analysis by tropospheric ties in GNSS and VLBI integrated processing. Journal of Geodesy, 2022, 96, 1.	3.6	10
75	Determination of a terrestrial reference frame via Kalman filtering of very long baseline interferometry data. Journal of Geodesy, 2016, 90, 1311-1327.	3.6	9
76	Improving the modeling of the atmospheric delay in the data analysis of the Intensive VLBI sessions and the impact on the UT1 estimates. Journal of Geodesy, 2017, 91, 857-866.	3.6	9
77	The impacts of source structure on geodetic parameters demonstrated by the radio source 3C371. Journal of Geodesy, 2017, 91, 767-781.	3.6	9
78	GPS/GLONASS Combined Precise Point Positioning With the Modeling of Highly Stable Receiver Clock in the Application of Monitoring Active Seismic Deformation. Journal of Geophysical Research: Solid Earth, 2018, 123, 4025-4040.	3.4	9
79	GNSS-based water vapor estimation and validation during the MOSAiC expedition. Atmospheric Measurement Techniques, 2021, 14, 5127-5138.	3.1	9
80	Improving the Vertical Modeling of Tropospheric Delay. Geophysical Research Letters, 2022, 49, .	4.0	9
81	Precise Onboard Real-Time Orbit Determination with a Low-Cost Single-Frequency GPS/BDS Receiver. Remote Sensing, 2019, 11, 1391.	4.0	8
82	Perturbations in atmospheric gaseous components over coastal Antarctica detected in GPS signals and its natural origin to volcanic eruption. Polar Science, 2019, 19, 69-76.	1.2	8
83	Integrated processing of ground- and space-based GPS observations: improving GPS satellite orbits observed with sparse ground networks. Journal of Geodesy, 2020, 94, 1.	3.6	8
84	Spatial and Temporal Distributions of Ionospheric Irregularities Derived from Regional and Global ROTI Maps. Remote Sensing, 2022, 14, 10.	4.0	8
85	Automatic Calibration of Process Noise Matrix and Measurement Noise Covariance for Multi-GNSS Precise Point Positioning. Mathematics, 2020, 8, 502.	2.2	7
86	Imaging VGOS Observations and Investigating Source Structure Effects. Journal of Geophysical Research: Solid Earth, 2021, 126, e2020JB021238.	3.4	7
87	Use of GNSS Tropospheric Products for Climate Monitoring (Working Group 3). , 2020, , 267-402.		7
88	Very long baseline interferometry: accuracy limits and relativistic tests. Proceedings of the International Astronomical Union, 2009, 5, 286-290.	0.0	6
89	Operational Multiâ€GNSS Global Ionosphere Maps at GFZ Derived From Uncombined Code and Phase Observations. Radio Science, 2021, 56, e2021RS007337.	1.6	6
90	A Priori Gradients in the Analysis of Space Geodetic Observations. International Association of Geodesy Symposia, 2013, , 105-109.	0.4	5

#	Article	IF	CITATIONS
91	Atmospheric modeling for co-located VLBI antennas and twin telescopes. Journal of Geodesy, 2015, 89, 655-665.	3.6	5
92	Multi-technique comparison of atmospheric parameters at the DORIS co-location sites during CONT14. Advances in Space Research, 2016, 58, 2758-2773.	2.6	5
93	Impact of the image alignment over frequency for the VLBI Global Observing System. Astronomy and Astrophysics, 2022, 663, A83.	5.1	5
94	Climatic signals observed by VLBI. Acta Geodaetica Et Geophysica Hungarica, 2006, 41, 159-170.	0.4	4
95	Long-Term Evaluation of Ocean Tidal Variation Models of Polar Motion and UT1. Pure and Applied Geophysics, 2018, 175, 1611-1629.	1.9	4
96	Evaluating the impact of higher-order ionospheric corrections on multi-GNSS ultra-rapid orbit determination. Journal of Geodesy, 2019, 93, 1347-1365.	3.6	4
97	A Comparative Study on the Solar Radiation Pressure Modeling in GPS Precise Orbit Determination. Remote Sensing, 2021, 13, 3388.	4.0	4
98	PPP Without Troposphere Estimation: Impact Assessment of Regional Versus Global Numerical Weather Models and Delay Parametrization. International Association of Geodesy Symposia, 2018, , 107-118.	0.4	3
99	Coastal sea-surface wave measurements using software-based GPS reflectometers in Lanyu, Taiwan. GPS Solutions, 2021, 25, 1.	4.3	3
100	Diagnostics of Es Layer Scintillation Observations Using FS3/COSMIC Data: Dependence on Sampling Spatial Scale. Remote Sensing, 2021, 13, 3732.	4.0	3
101	Modelling Very Long Baseline Interferometry (VLBI) observations. Journal of Geodesy and Geoinformation, 2012, 1, 17-26.	0.2	3
102	The Potsdam Open Source Radio Interferometry Tool (PORT). Publications of the Astronomical Society of the Pacific, 2021, 133, 104503.	3.1	3
103	Future GNSS Infrastructure for Improved Geodetic Reference Frames. , 2020, , .		3
104	Inter-Comparison of UT1-UTC from 24-Hour, Intensives, and VGOS Sessions during CONT17. Sensors, 2022, 22, 2740.	3.8	3
105	Using VLBI fringe-phase information from geodetic experiments for short-period ionospheric studies. Journal of Geodesy, 2007, 81, 389-401.	3.6	2
106	Short-term tidal variations in UT1: compliance between modelling and observation. Proceedings of the International Astronomical Union, 2009, 5, 215-215.	0.0	2
107	The Role of Spatial Gradient on Vertical Total Electron Content Extraction From Geodetic Very Long Baseline Interferometry Observation: Case Study CONT08 to CONT17‣1. Space Weather, 2021, 19, e2020SW002633.	3.7	2
108	Towards Understanding the Interconnection between Celestial Pole Motion and Earth's Magnetic Field Using Space Geodetic Techniques. Sensors, 2021, 21, 7555.	3.8	2

#	Article	IF	CITATIONS
109	Stability analysis of the Iraqi GNSS stations. Journal of Applied Geodesy, 2022, 16, 299-312.	1.1	2
110	Fast BDS Positioning Convergence Based on the Contribution of GPS Observations. Marine Geodesy, 2017, 40, 404-415.	2.0	1
111	Editorial note for the Geodesy and Geodynamics journal special issue. Geodesy and Geodynamics, 2018, 9, 183-186.	2.2	1
112	Evaluation of VLBI Observations with Sensitivity and Robustness Analyses. Mathematics, 2020, 8, 939.	2.2	1
113	Drift of the Earth's Principal Axes of Inertia from GRACE and Satellite Laser Ranging Data. Remote Sensing, 2020, 12, 314.	4.0	1
114	An analysis of a priori and empirical solar radiation pressure models for GPS satellites. Advances in Geosciences, 0, 55, 33-45.	12.0	1
115	Temporal changes in atmospheric water content during the December 2004 Sumatra earthquake as estimated from GPS signals and its possible connection to the January 2005 California flash flood. Annals of Geophysics, 2018, 61, .	1.0	1
116	GGOS Bureau of Products and Standards: Description and Promotion of Geodetic Products. International Association of Geodesy Symposia, 2022, , .	0.4	1
117	Determination of UT1 by VLBI. Proceedings of the International Astronomical Union, 2009, 5, 216-216.	0.0	0
118	Alternative Approach for Tsunami Early Warning Indicated by Gravity Wave Effects on Ionosphere. Remote Sensing, 2021, 13, 2150.	4.0	0